Gamma-ray Emission from Pulsar Outer Magnetospheres

Kouichi HIROTANI

ASIAA/TIARA

Aspen workshop on GeV and TeV Sources
June 16, 2010

Crab nebula: Composite image of X-ray [blue] and optical [red]

§1 Introduction: The γ-ray sky

After 2008, *LAT* aboard *Fermi space telescope* has detected 46 (+9) pulsars above 100 MeV.

Fermi/LAT point sources (>100 MeV)

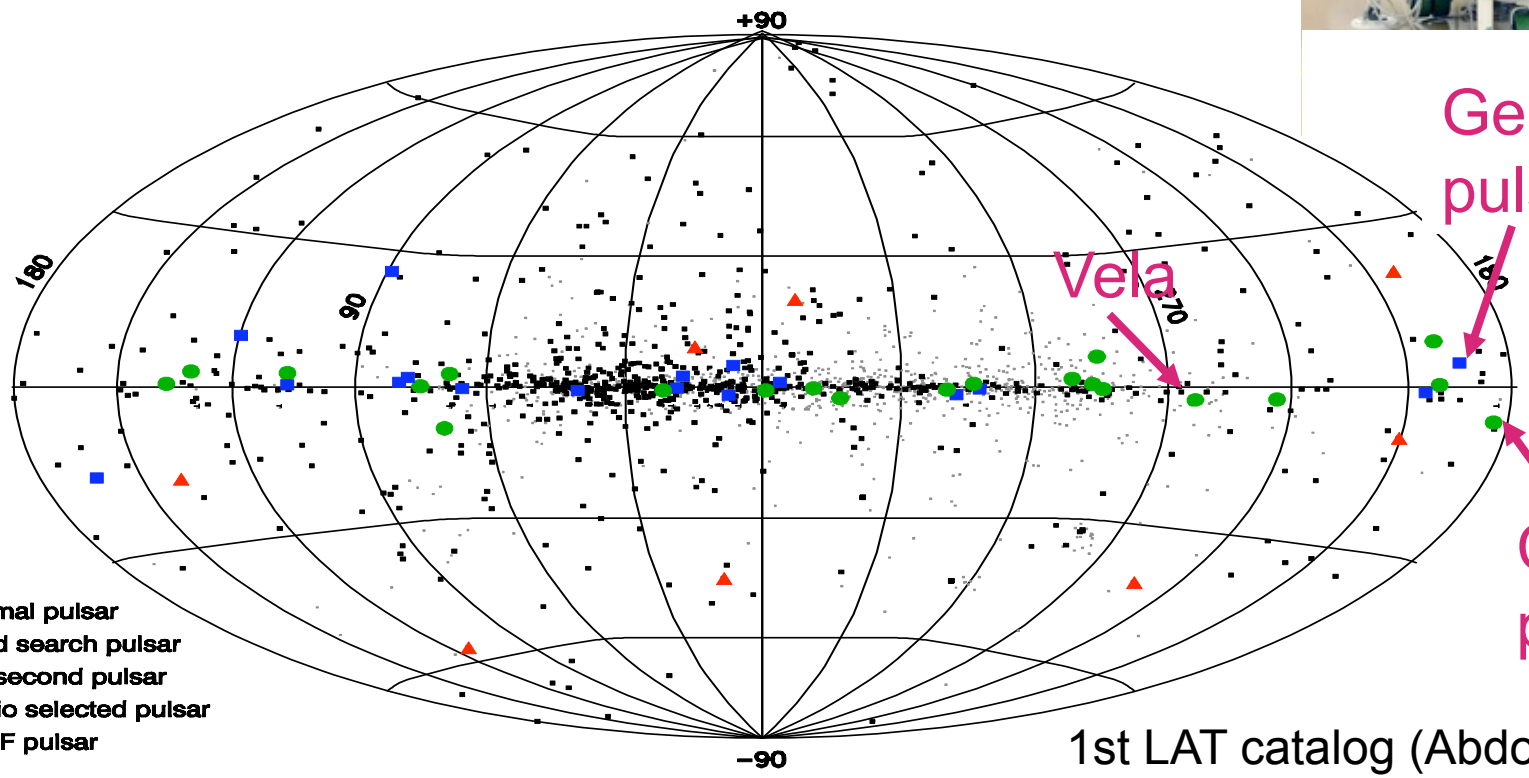

Geminga pulsar

Vela

Crab pulsar

1st LAT catalog (Abdo+ 2009)

§1 γ-ray Observations of Pulsars

Their light curves typically exhibit double-peak pulse profiles.

(34 among 46 *LAT* pulsars)

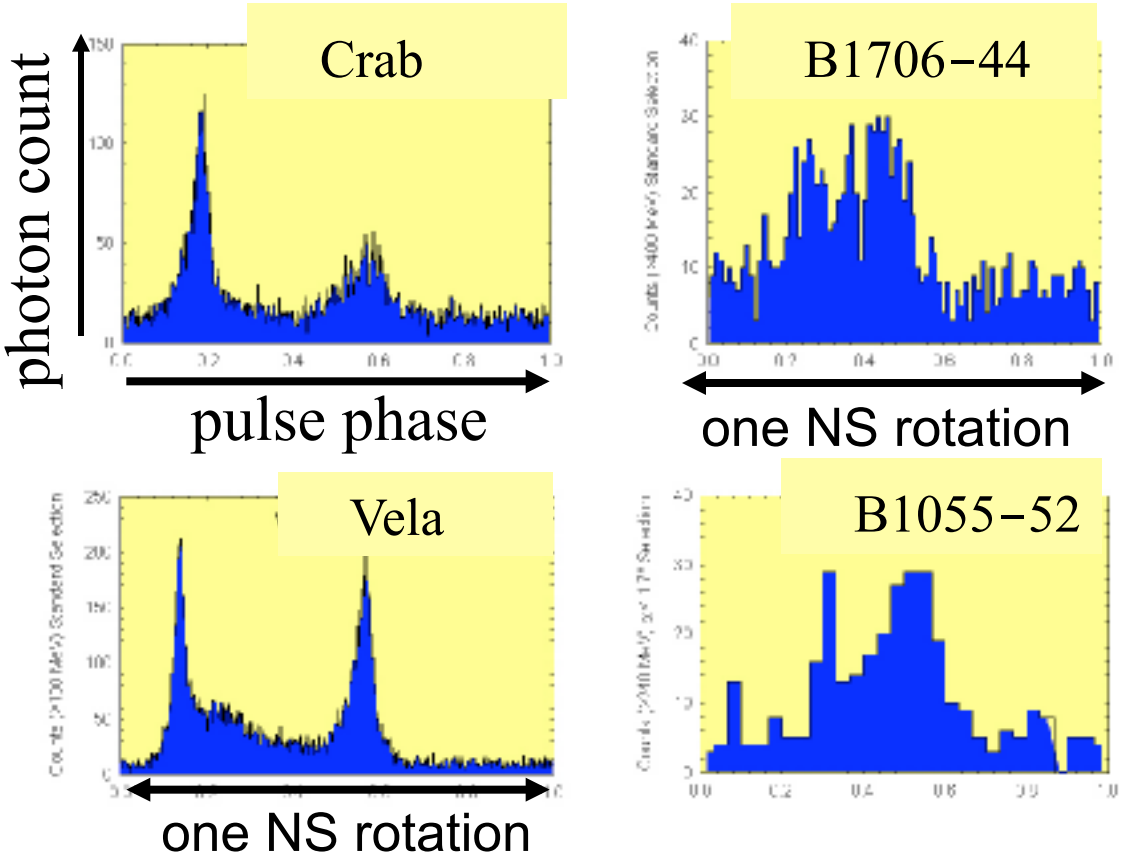

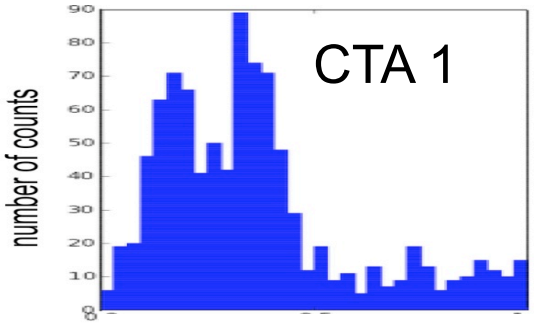

LAT (Abdo+ 08)

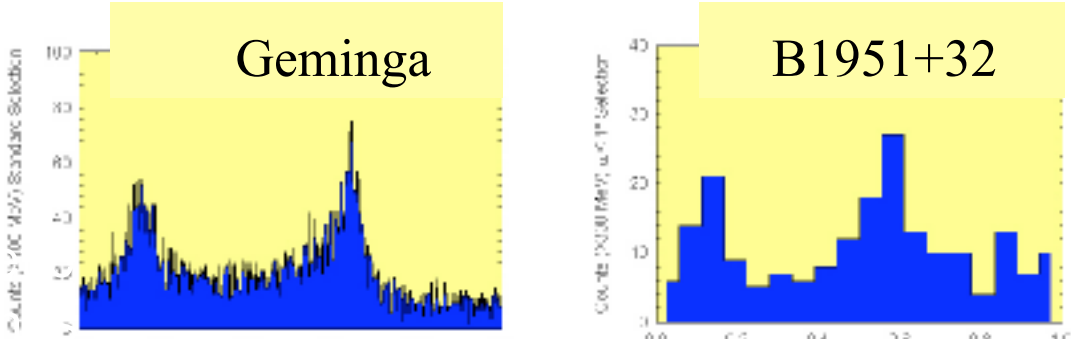

EGRET (Thompson 01, Kanbach 02)

Broad-band spectra (pulsed)

- High-energy (>100MeV) photons are emitted via **curvature** process by ultra-relativistic (~10 TeV) $e^{\pm}$'s accelerated in pulsar magnetosphere.

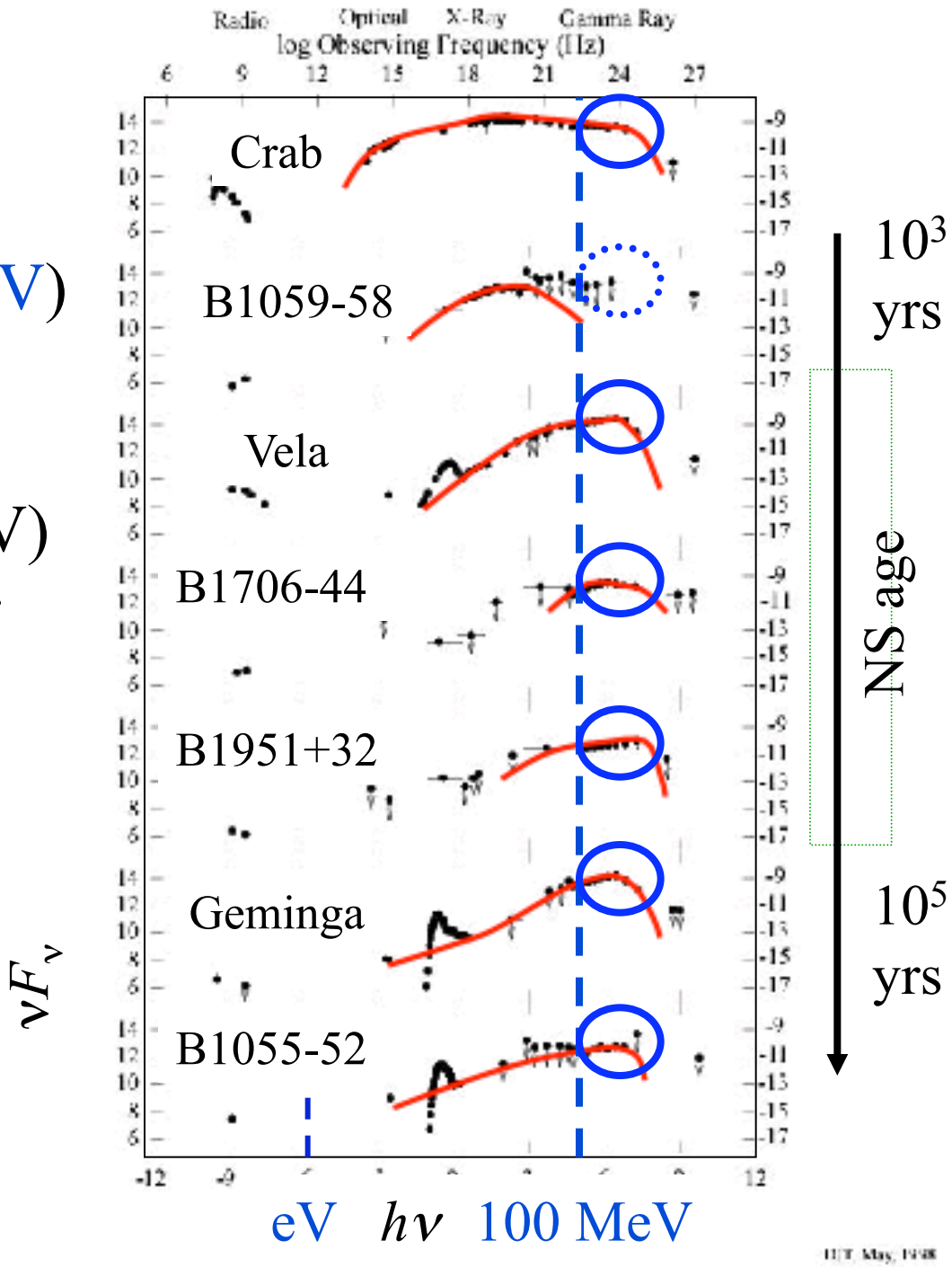

§ 2 *Previous Models*

Early 80's, polar-cap (PC) model was proposed.

(Daugherty & Harding ApJ 252, 337, 1982)

Emission altitude $< 3r_{NS}$ ⟶ pencil beam ($\Delta\Omega$ «1 ster)

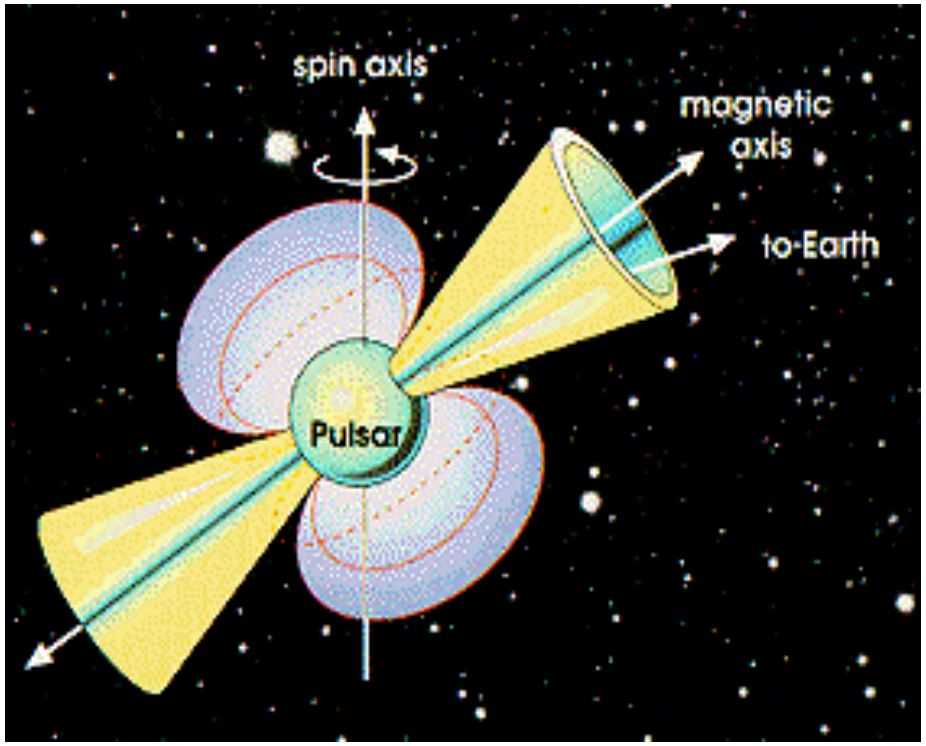

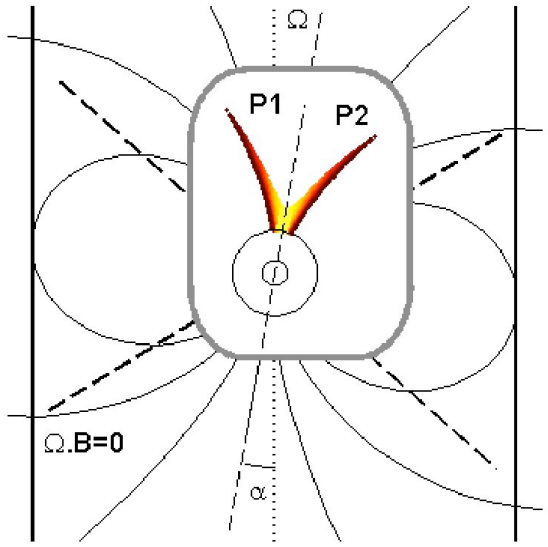

Grenier & Harding (2006)

Difficult to reproduce wide-separated double peaks.

⟶ High-altitude emission drew attention.

§ 2 *Previous Models*

Mid 80's, outer-gap (OG) model was proposed.

(Cheng, Ho, Ruderman ApJ 300, 500, 1986)

Emission altitude > 100 r_{NS} ⟶ hollow cone emission ($\Delta\Omega > 1$ ster)

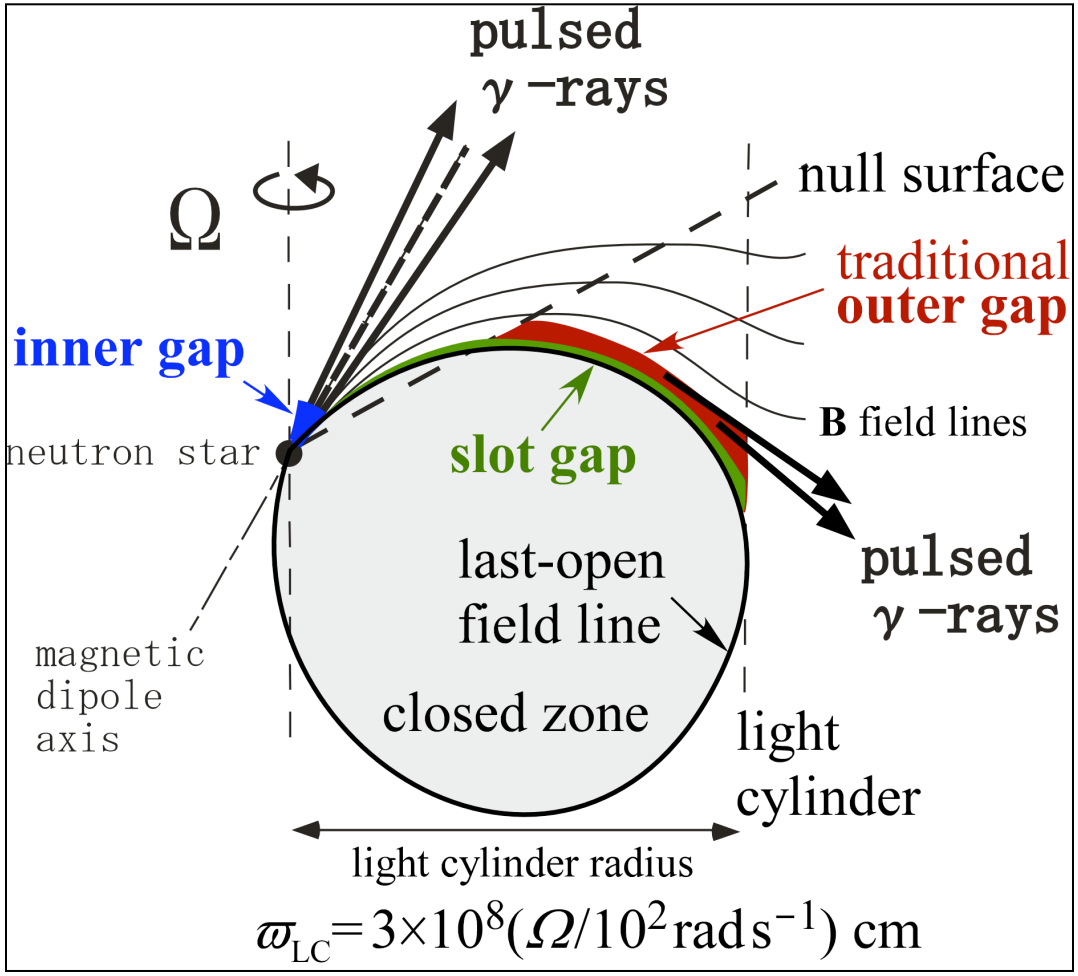

§ 2 *Previous Models*

Mid 80's, outer-gap (OG) model was proposed.

(Cheng, Ho, Ruderman ApJ 300, 500, 1986)

Emission altitude > 100 r_{NS} ⟶ hollow cone emission ($\Delta\Omega > 1$ ster)

Mid 90s', the outer-gap model was further developed by taking account of special relativistic effects.

(Romani ApJ 470, 469, 1995)

⟶ Explains wide-separated double peaks.

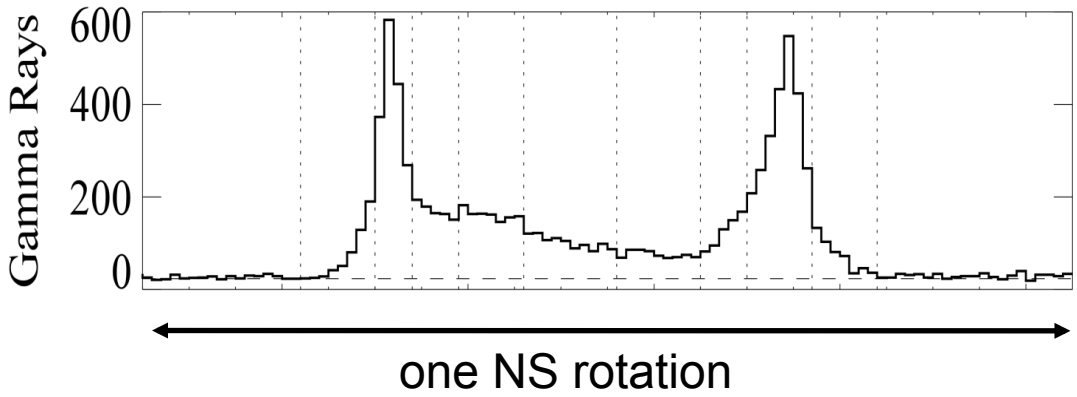

§ 2 *Previous Models*

Mid 80's, outer-gap (OG) model was proposed.

(Cheng, Ho, Ruderman ApJ 300, 500, 1986)

Emission altitude > 100 r_{NS} ⟶ hollow cone emission ($\Delta\Omega > 1$ ster)

Mid 90s', the outer-gap model was further developed by taking account of special relativistic effects.

(Romani ApJ 470, 469)

⟶ Explains wide-separated double peaks.

OG model became promising as HE emission model.

§ 2 *Previous Models*

However, the original, geometrically thin OG model cannot reproduce the observed γ-ray flux.

Hirotani (2008) ApJ 688, L25

In addition, the same difficulty applies to an alternative, thin Pair-Starved Polar-Cap model (Harding+2008).

On these grounds, all the pulsar emission models adopt transversely thick accelerator geometry.
(e.g., thick OG model/thick PSPC model)

Nest question: Can a thick OG produce sharp peaks?

Answer: YES!! ⟵ Today's topic.

§ 3 New gap theory: Self-consistent approach

How to construct a self-consistent particle accelerator theory in pulsar magnetospheres.

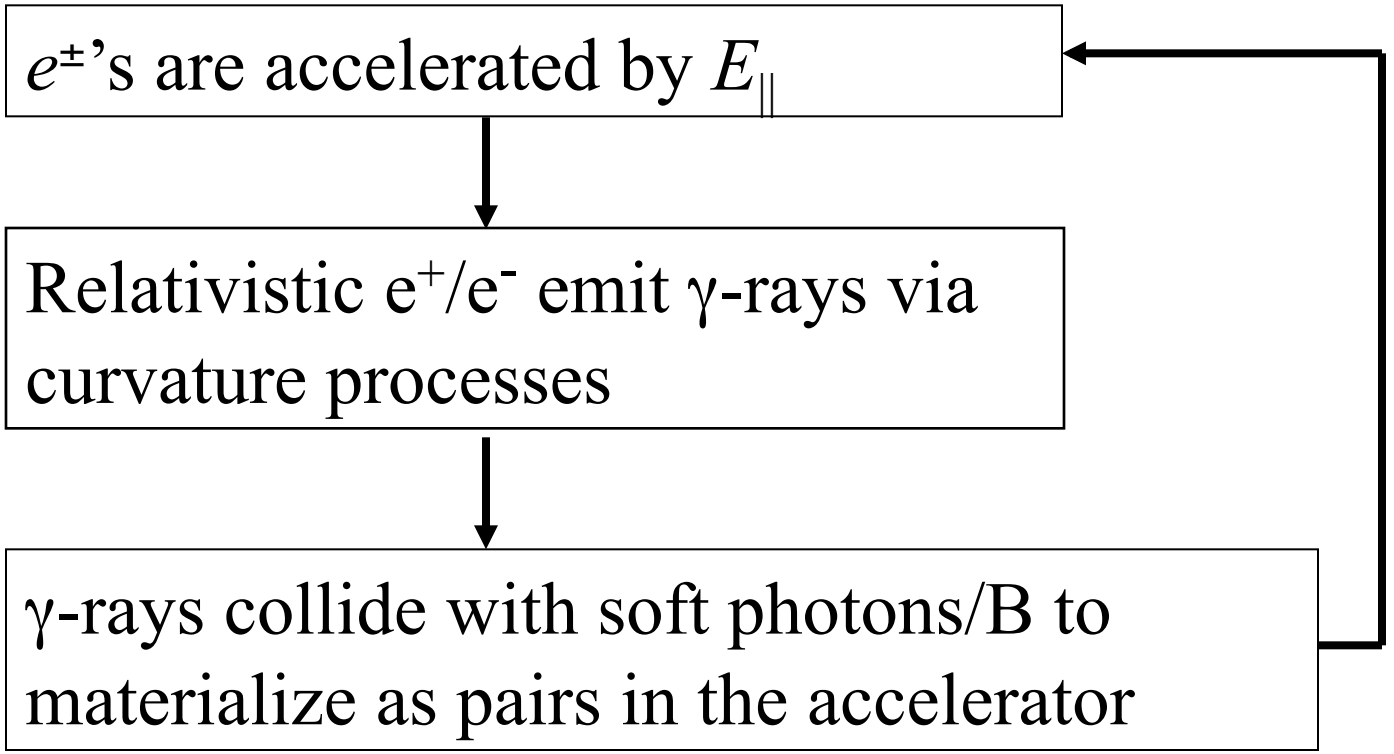

§ 3 New gap theory: Self-consistent approach

The Poisson equation for the electrostatic potential ψ is given by

$$-\nabla^2\psi = 4\pi(\rho - \rho_{\rm GJ}) ,$$

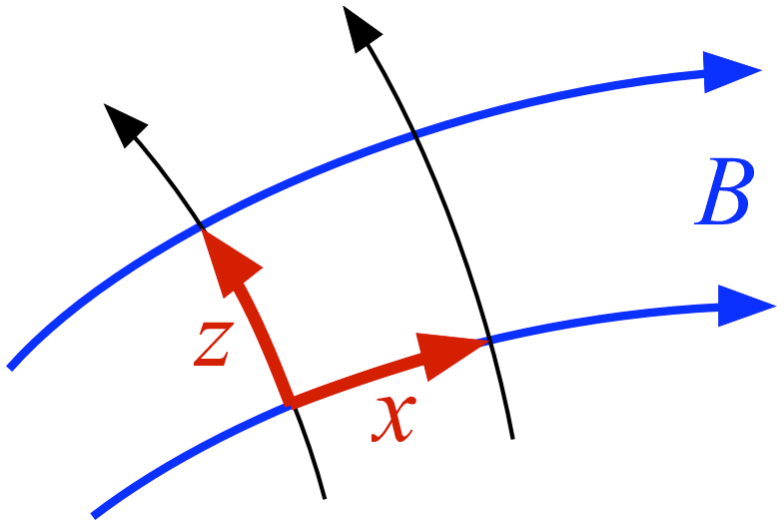

where

$$E_{\parallel} \equiv -\frac{\partial \Psi}{\partial x} ,$$

$$\rho \equiv e\int_0^{\infty} d\Gamma\left[N_+(x,y,z,\Gamma,\chi) - N_-(x,y,z,\Gamma,\chi)\right] + \rho_{\rm ion} ,$$

$$\rho_{\rm GJ} \equiv -\frac{\mathbf{\Omega B}}{2\pi c} .$$

N_+/N_-: distribution function of e^+/e^-

Γ: Lorentz factor of e^+/e^-

χ : pitch angle of e^+/e^-

§ 3 New gap theory: Self-consistent approach

Assuming $\partial_t+\Omega\partial_\phi=0$, we solve the $e^{\pm}$'s Boltzmann eqs.

$$\frac{\partial N_{\pm}}{\partial t}+\vec{v}\cdot\nabla N_{\pm}+\left(e\overrightarrow{E_{\parallel}}+\frac{\vec{v}}{c}\times\overrightarrow{B}\right)\cdot\frac{\partial N_{\pm}}{\partial\overrightarrow{p}}=S_{IC}+\int\alpha_{\nu}d\nu\int\frac{I_{\nu}}{h\nu}d\omega$$

together with the radiative transfer equation,

$$\frac{dI_{\nu}}{dl}=-\alpha_{\nu}I_{\nu}+j_{\nu}$$

$N_{\pm}$: distribution function of e^+/e^-,
$E_{\parallel}$: mangnetic-field-aligned electric field,
$S_{\rm IC}$: ICS re-distribution function, $d\omega$: solid angle element,
I_{ν}: photon specific intensity, l : path length along the ray
α_{ν}: absorption coefficient, j_{ν}: emission coefficient

§ 3 New gap theory: Self-consistent approach

To solve the set of Poisson, Boltzmann, radiative-transfer eqs. in 6-D phase space, we have to specify the following three parameters: (period P: observable)

- magnetic inclination (e.g., $\alpha_{\rm inc}$=45°, 75°),
- magnetic dipole moment of NS (e.g., μ=4×10^{30}G cm^3)
- neutron-star surface temperature (e.g., $kT_{\rm NS}$=50 eV)

I first solved

- gap geometry in 3-D pulsar magnetosphere,
- spatial distribution of acceleration electric field, $E_{||}$,
- distribution functions of $e^{\pm}$'s,
- specific intensity of emitted photon field (IR-VHE),

by specifying these three parameters.

§ 4 Results

This method can be applied to arbitrary pulsars.

Today's topic:

Crab, Vela (10^3 ~10^4 yrs) : Does the copious pair production affect the gap structure? Does the screened gap reproduce observations?

Geminga (~10^5 yrs): Does a thick gap produces double sharp peaks?

§ 4 Self-consistent gap solution: Crab

3-D distribution of the particle accelerator (i.e., high-energy emission zone) is solved from the Poisson eq.

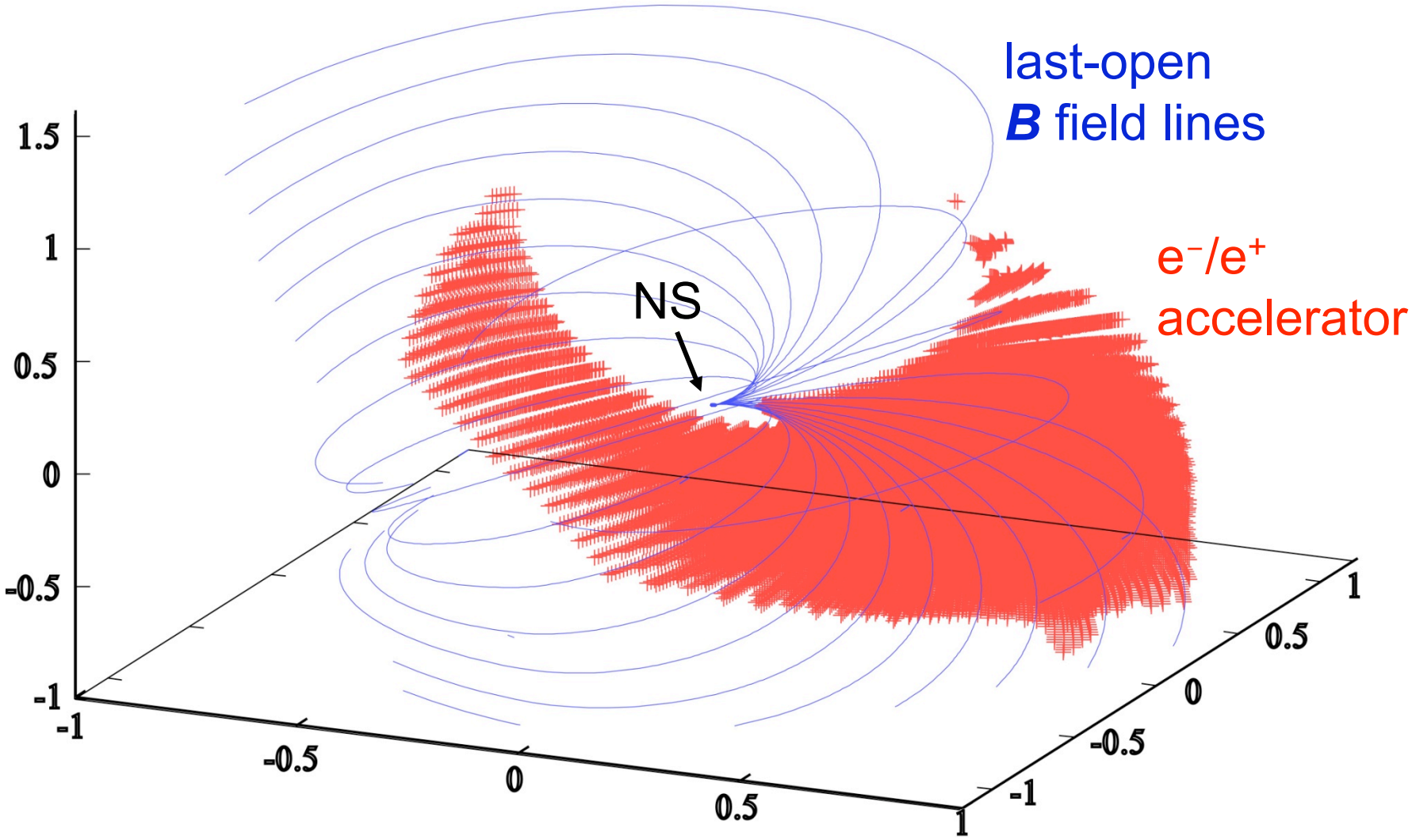

§ 4 Self-consistent gap solution: Crab

The gap activity is controlled by f^3.

meridional thickness, $f = f(s, \phi)$. [ϕ: magnetic azimuth]

■ Previous models: estimate f by dimension analysis.

■ This work: solve f from the basic equations in 3-D magnetosphere.

§ 4 Self-consistent gap solution: Crab

The gap activity is controlled by f^3.

meridional thickness, $f = f(s, \phi)$. [ϕ: magnetic azimuth]

Self-consistent solution for the Crab case:

Fig.) gap trans-field thickness on 2-D last-open-field-line surface

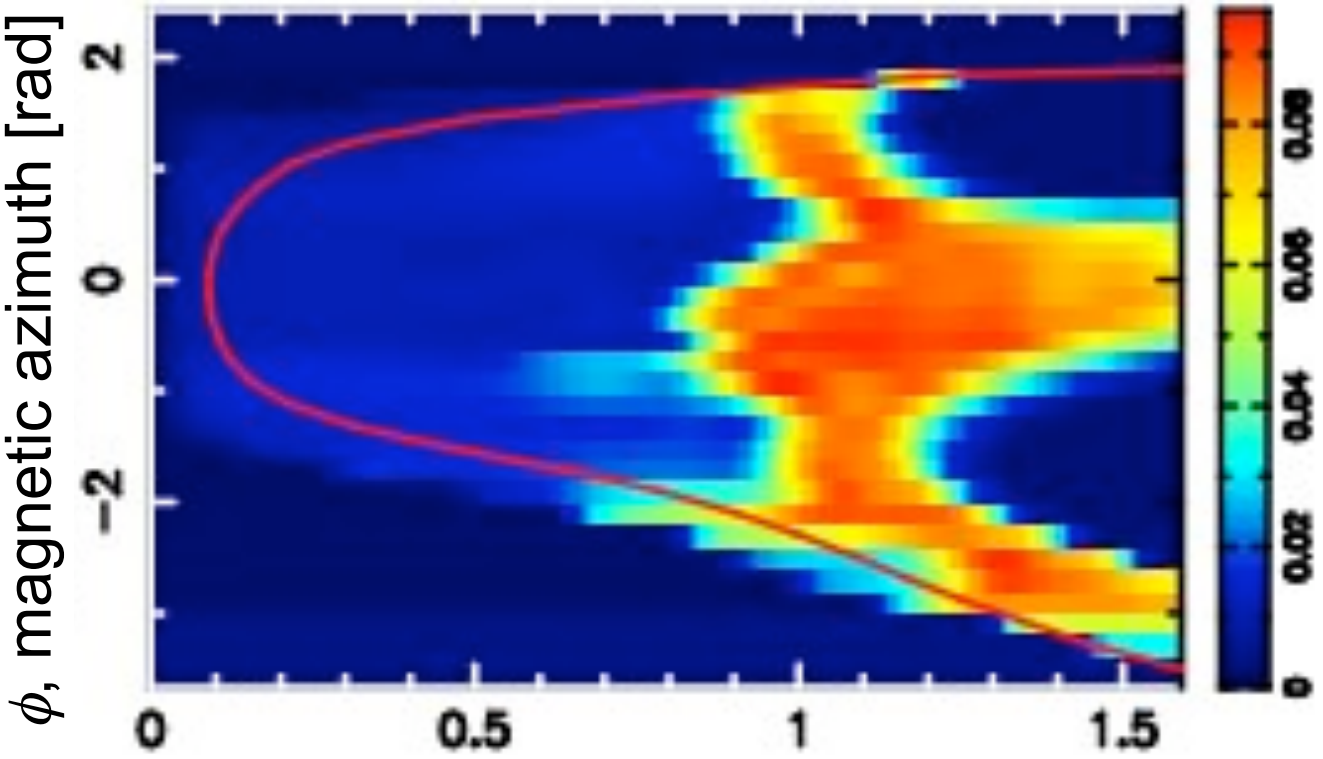

§ 4 Self-consistent gap solution: Crab

Intrinsic quantities (e.g., gap 3-D geometry, f, $E_{||}$, $e^{\pm}$ distribution functions, specific intensity at each point) of an OG are now self-consistently solved if we specify ***B*** inclination, NS magnetic moment, NS surface temperature, without introducing any artificial assumptions.

If we additionally give the distance and observer's viewing angle, we can predict the luminosity, pulse profiles, and the photon spectrum in each pulse phase.

§ 4 *Self-consistent gap solution: Crab*

Photons are emitted along the local ***B*** field lines (in the co-rotating frame) by relativistic beaming and propagate in a hollow cone.

The hollow cone emission is projected on the 2-D propagation directional plane.

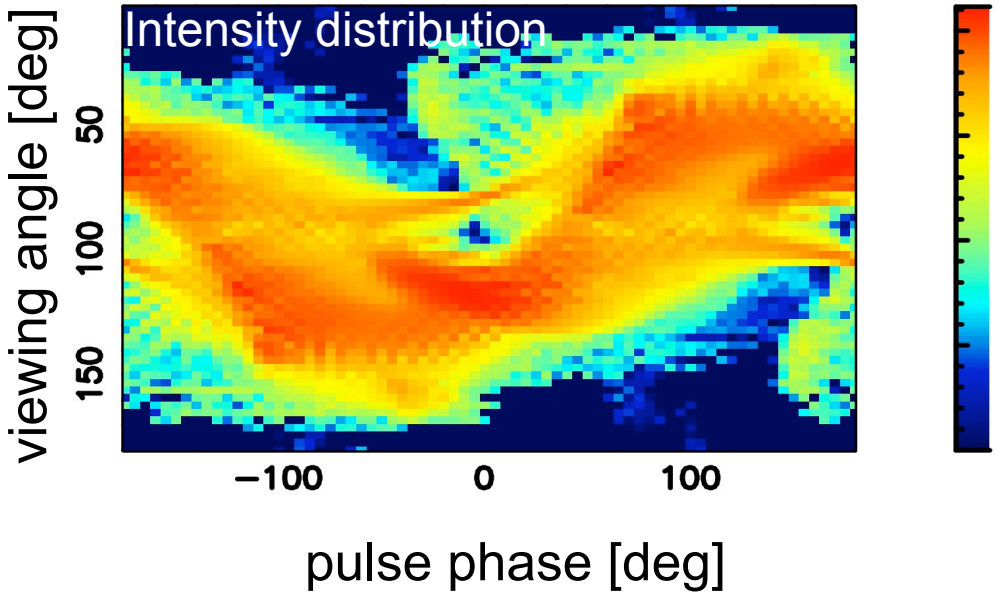

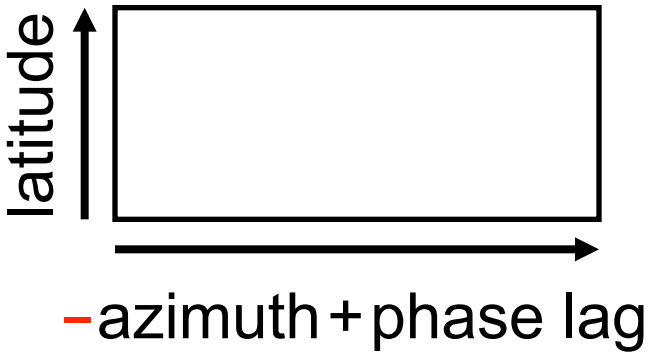

one NS rotation

Photons emitted at smaller azimuth arrives earlier.

§ 4 Self-consistent gap solution: Crab

Photons are emitted along the local ***B*** field lines (in the co-rotating frame) by relativistic beaming and propagate in a hollow cone.

The hollow cone emission is projected on the 2-D propagation directional plane.

If we specify the observer's viewing angle, we obtain the pulse profile.

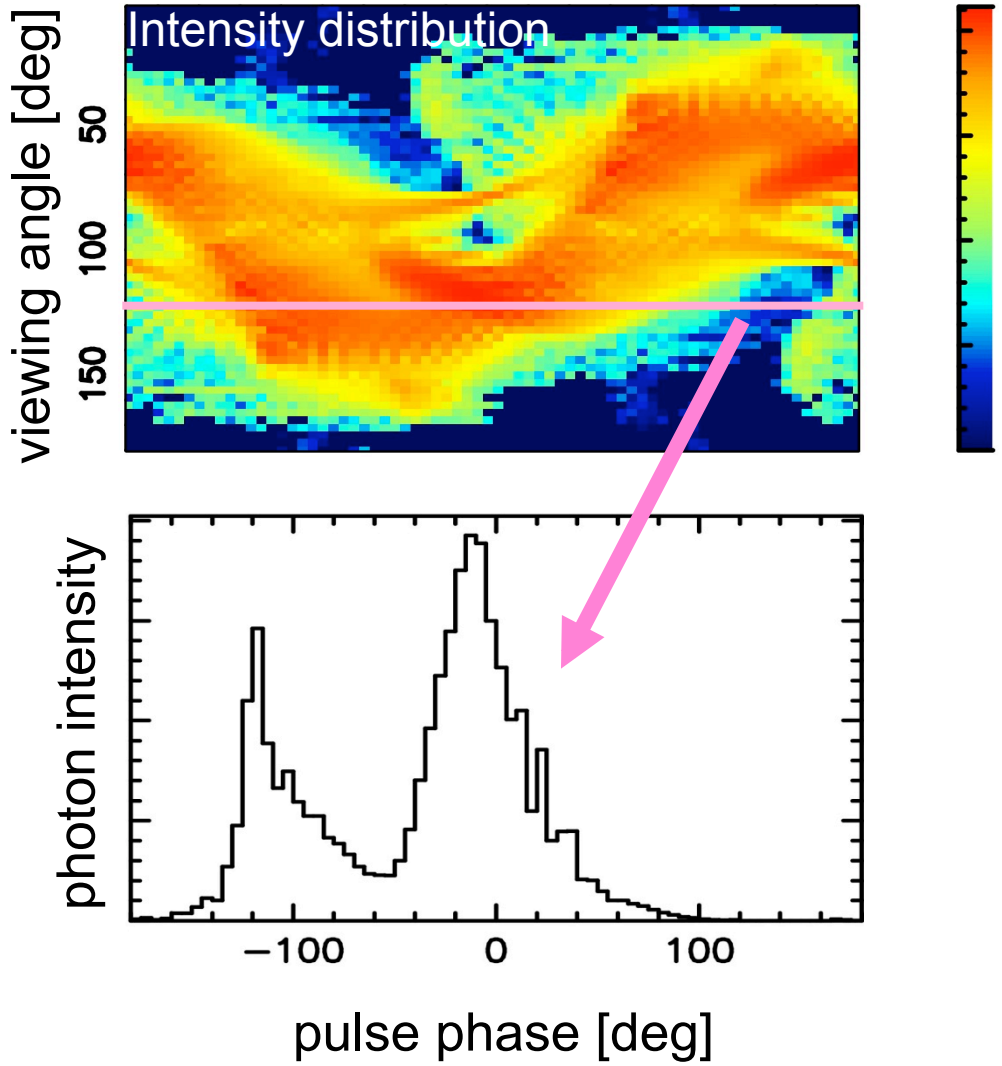

§ 4 Self-consistent gap solution: Crab

Predicted spectra reproduce observations, if we assume appropriate viewing angle (e.g., ~100°).

Fig.) OG prediction of Crab νF_ν spectra

solid:
un-abs. primary

dashed:
un-abs. 2ndary

red:
to be observed,
prim.+2nd+3rd

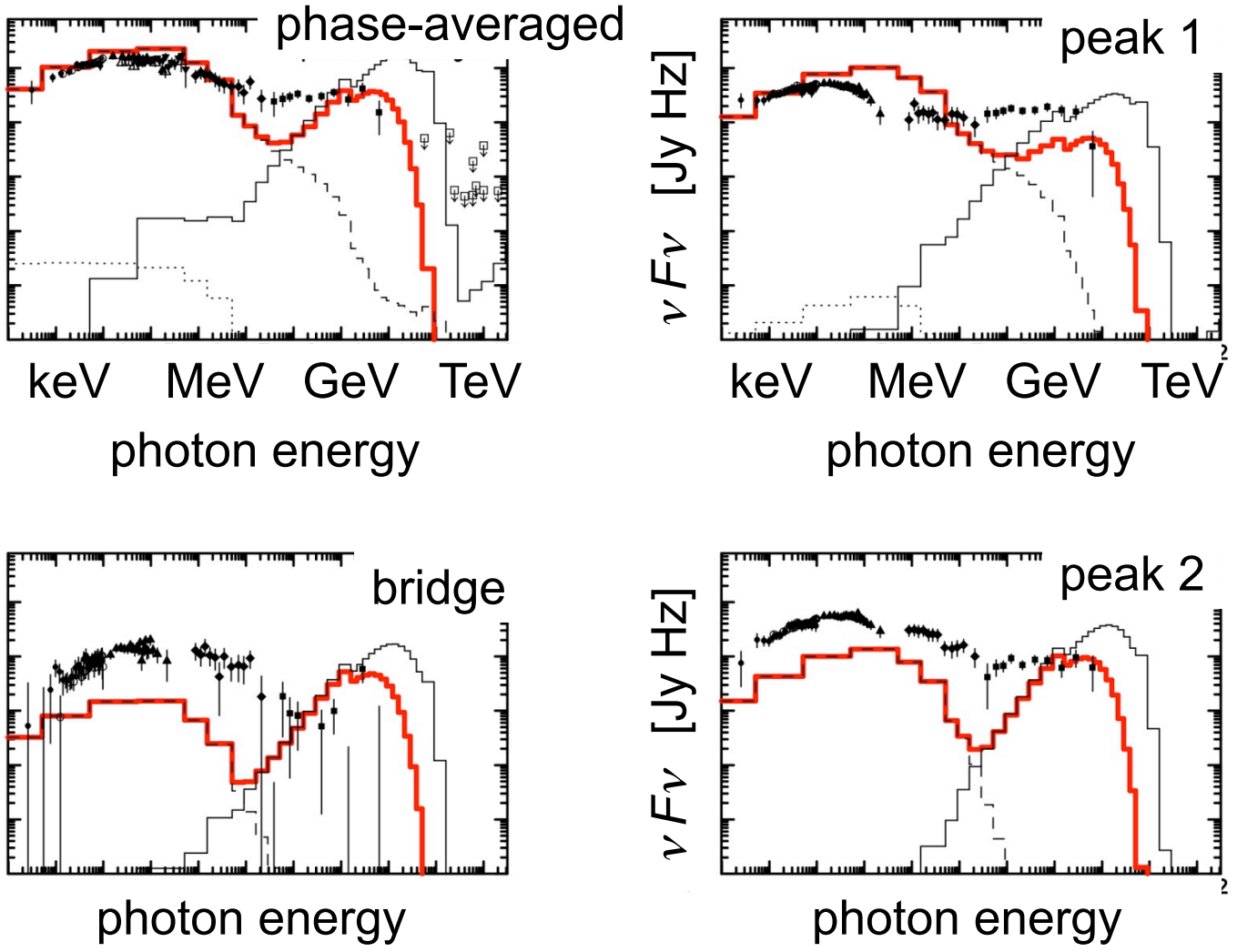

§ 4 Self-consistent gap solution: Vela

Vela case: *γ−γ pair production also regulates f(s,ϕ).*

LS suffers substantial E-field screening due to pair production. (more prominent than Crab)

f(s,ϕ) distribution (i.e., 3-D gap geometry)

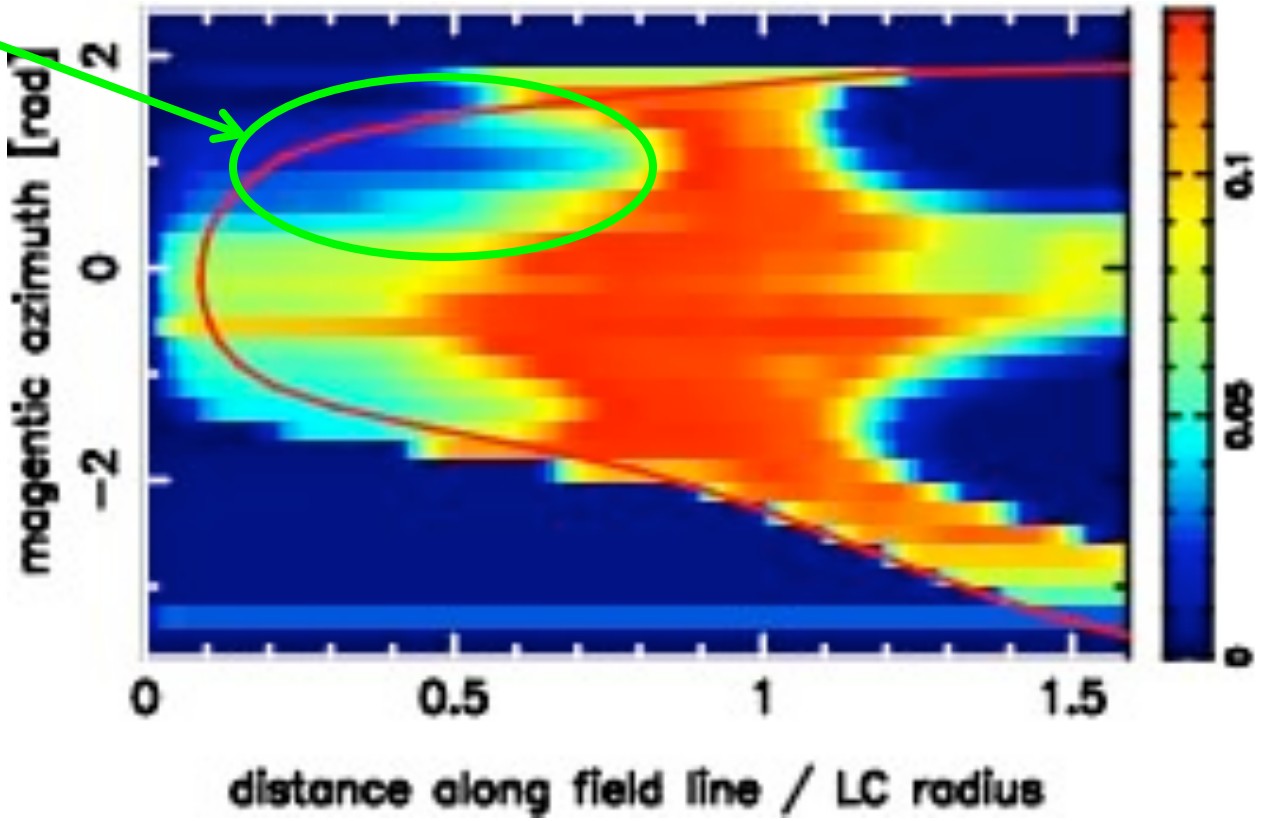

§ 4 Self-consistent gap solution: Vela

Vela pulsar also exhibits primary VHE component (~0.2% of νF_ν peak), because of the ICS by gap-accelerated e^+'s in the wind (near the light cylinder).

However, the VHE component is totally absorbed by the same soft photon field (IR-UV), in the same way as Crab.

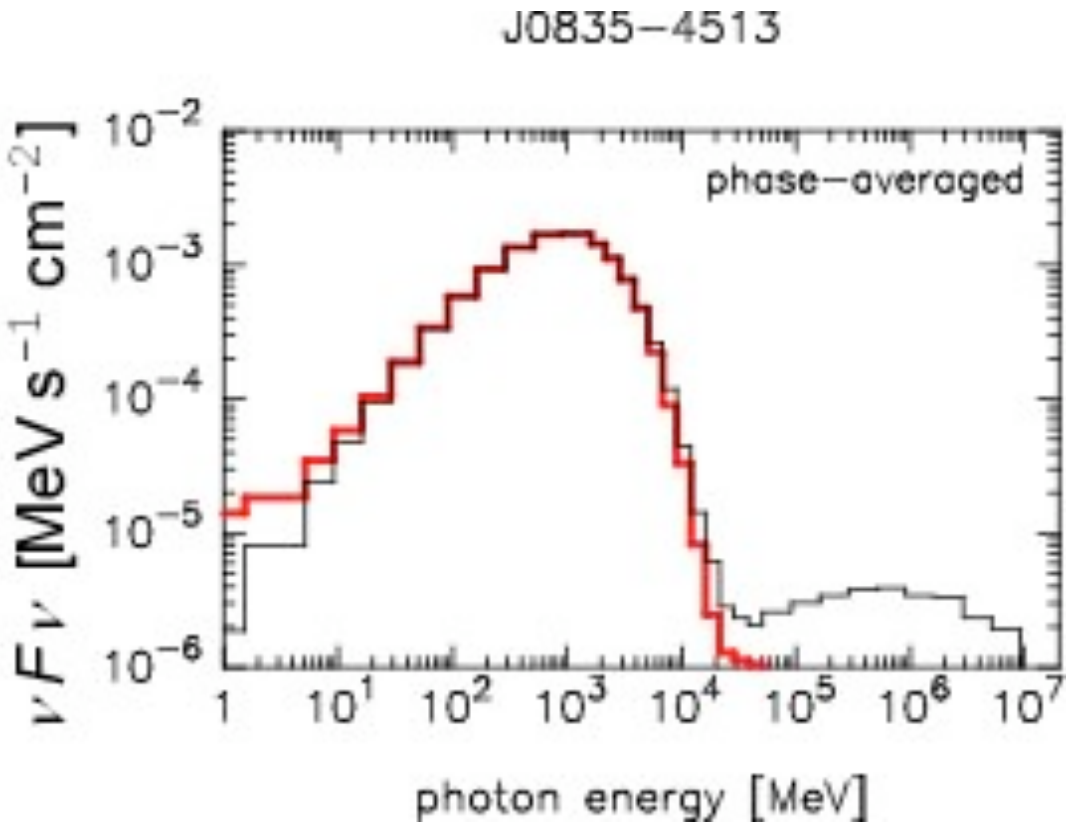

§ 4 Self-consistent gap solution: Geminga

Gap trans-field thickness is regulated (and $E_{||}$ is screened) by the discharge of produced pairs.

Ex: Geminga pulsar

$\mu = 2\mu_{\rm dipole}$

Screening due to pair production.

Double-peak light curve

Trans-field thickness plotted on the last-open field line surface

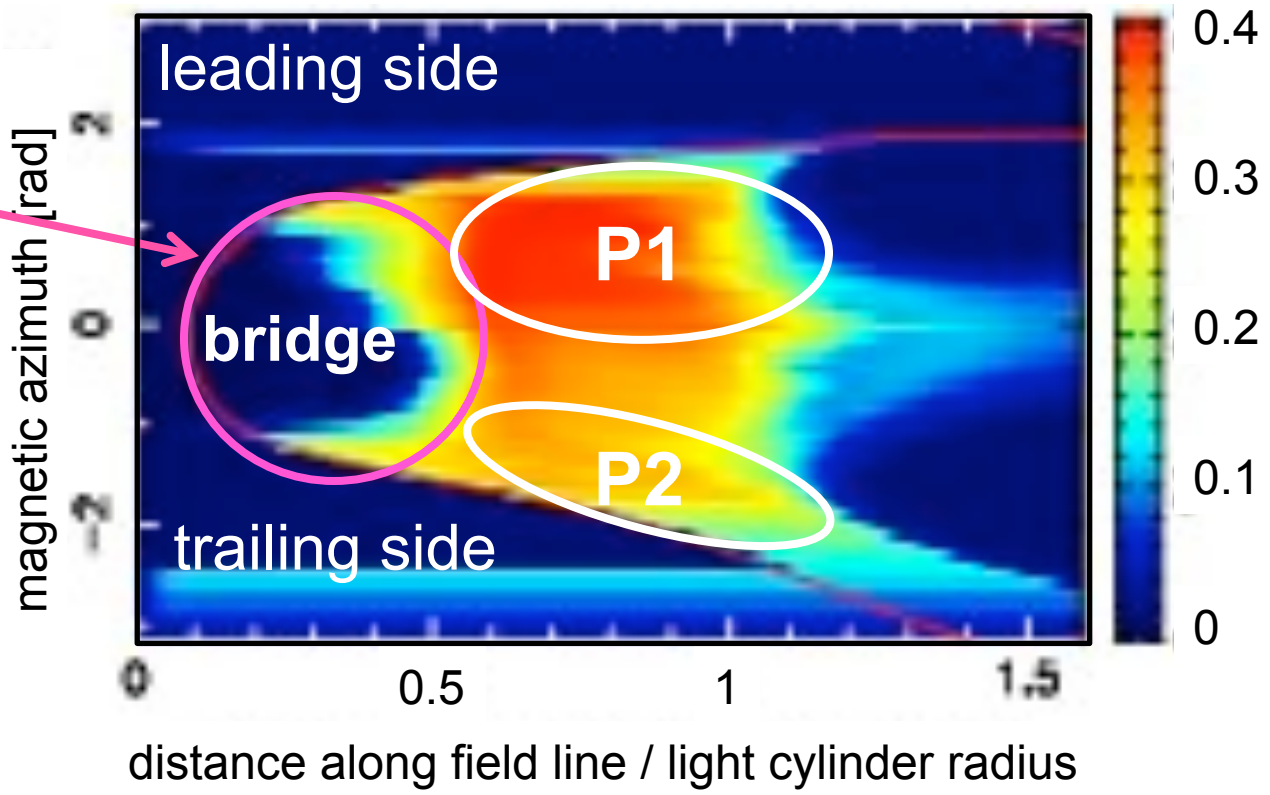

§ 4 *Self-consistent gap solution: Geminga*

Geminga pulsar

Photon plot on phase diagram:

Double-peak light curve is formed by the $E_{||}$ screening due to γ-γ pair production at lower altitudes.

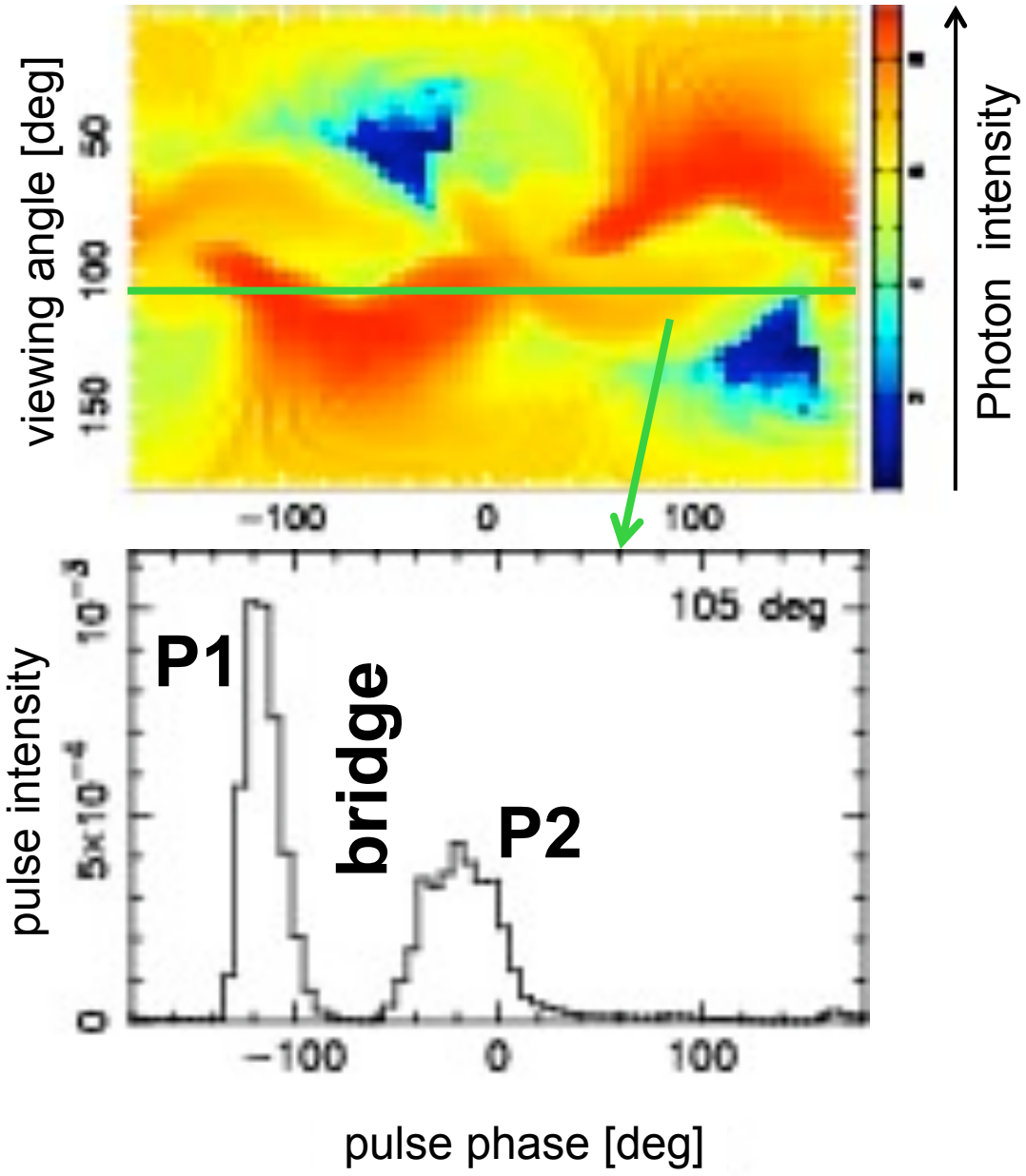

§ 4 *Self-consistent gap solution: Geminga*

Created electric current relatively concentrates along limited ***B*** flux tubes.

Light-curve peak becomes relatively sharp.

(Thanks, Isabelle.)

Polar-cap surface (Geminga)

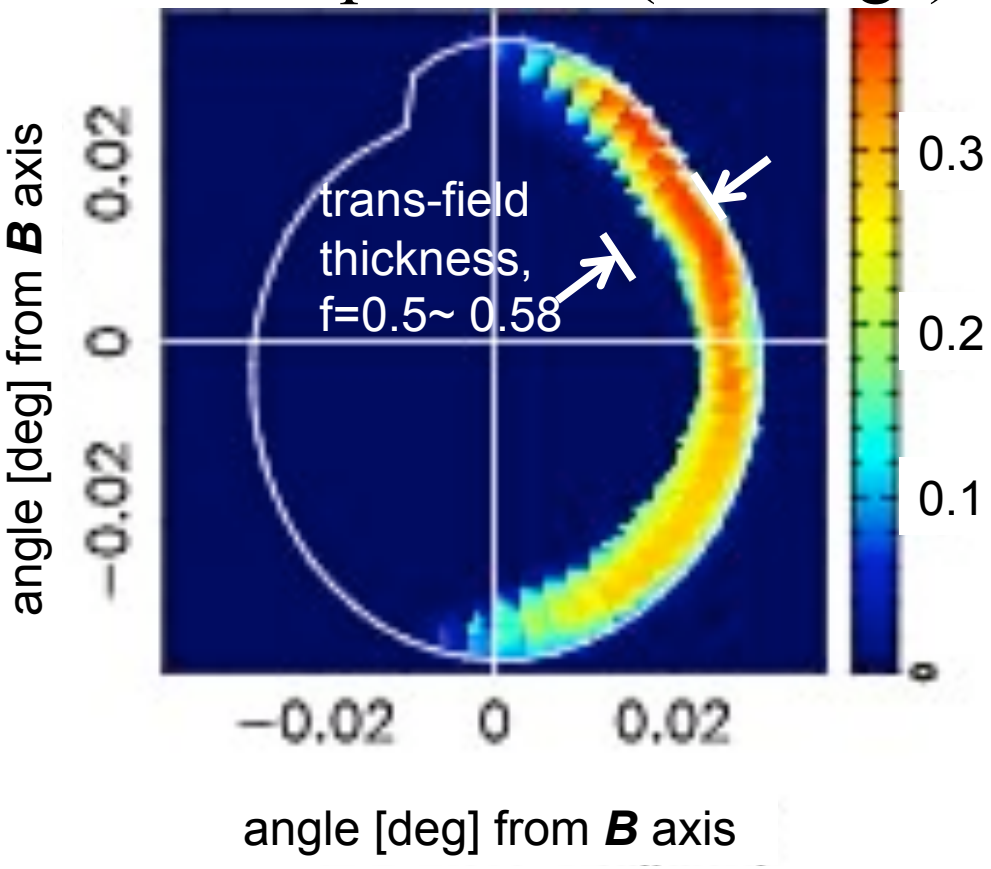

Summary

- We can solve pulsar high-energy emission zones (i.e., gaps) from the set of Maxwell (div$\boldsymbol{E}=4\pi\rho$ only), Boltzmann, and radiative-transfer eqs., by specifying P, dP/dt, $\alpha_{\rm incl}$, $kT_{\rm NS}$. We no longer have to assume the gap geometry, $E_{||}$, $e^{\pm}$ distribution functions. $\boldsymbol{B}$ field is assumed to be given by a rotating vacuum dipole field.

- The gap solution corresponds to a quantitative extension of the phenomenological OG models, and qualitatively reproduces such as observed pulse profiles, phase-resolved spectra from IR to VHE.

- Although the Geminga pulsar has a thick gap, it reproduces relatively sharp peaks that are observed.

Questions for discussion

- Crab's OG is active only in the higher altitudes due to strong $E_{\parallel}$ screening. → Easily subject to $\boldsymbol{B}$ modification.
- Conjecture: Vela's P3 is formed by the unscreened $E_{\parallel}$ near $\boldsymbol{\Omega}$-μ plane. ← Now examining with higher accuracy.
- No solution exists for Geminga if $\mu=\mu_{\rm dipole}$. That is, Geminga-like pulsars easily fall in the OG death valley (e.g, by strengthening of $\boldsymbol{B}$ in the higher altitudes).
- However, without an OG, the PC may supply copious plasmas, which eventually flow out as a pulsar wind.
- Thus, there many be many outer-gap-inactive, pulsar-wind active middle-aged/old pulsars (nearby). That is, there may be many γ-ray dim pulsars with wind activities.
- Applying the same method, distance to γ-ray only pulsars can be inferred.

§ 1 γ-ray Observations of Pulsars

Double-peak pulse profile is common.

(34 among 46 *LAT* pulsars)

Peak separation is typically between 100° and 180°.

Peak separation has no strong dependence on pulsar age (i.e., E_{spin}).

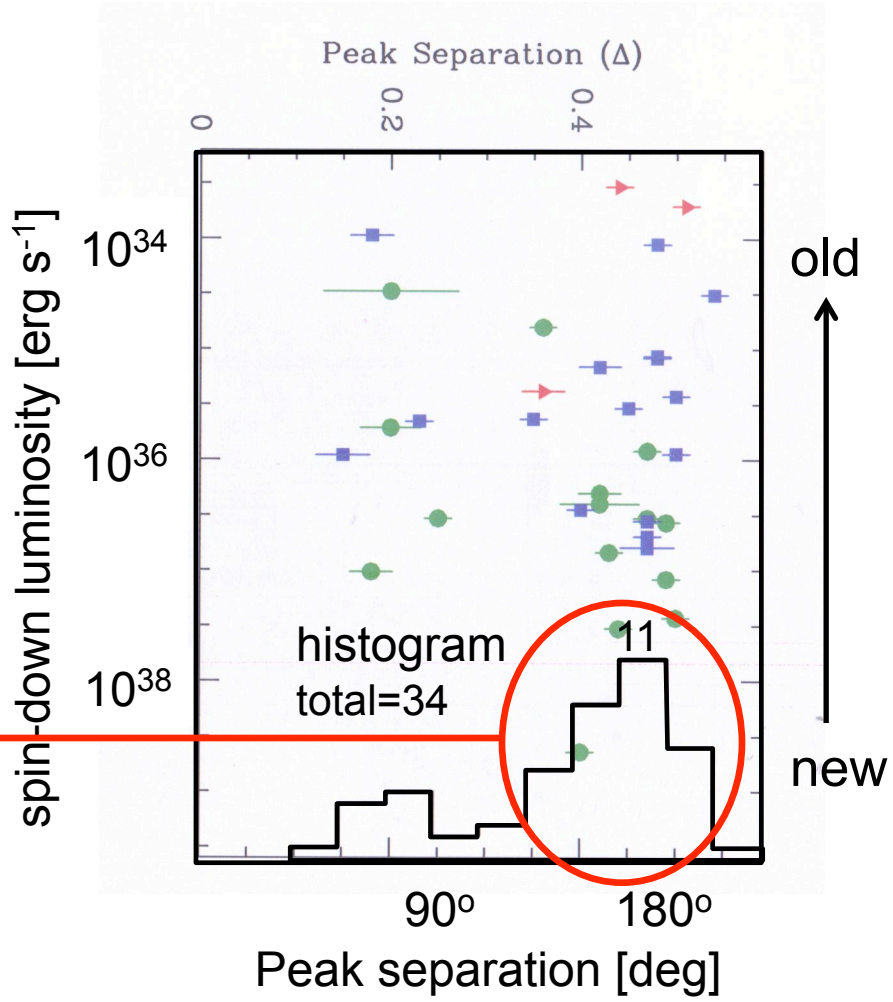

1st LAT catalog (Abdo+ 2009)

Broad-band spectra (pulsed)

- Power peaks in γ-rays
- No pulsed emission above 50 GeV
- High-energy turnover
- Spectrum gets harder as the NS ages. E.g., the **Crab** pulsar shows very soft γ-ray spectrum.
- B1951+32 shows the hardest spectrum.

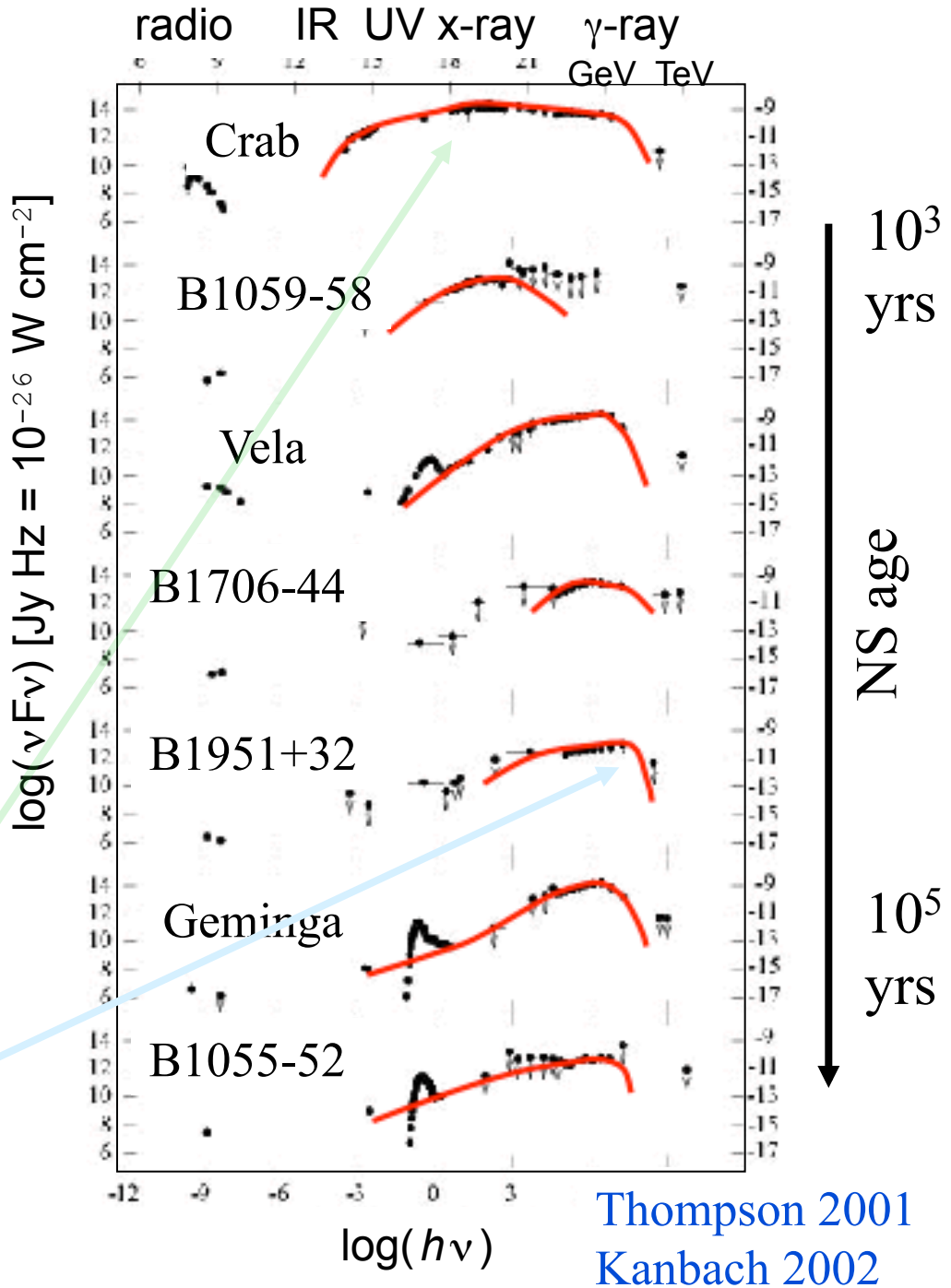

Thompson 2001
Kanbach 2002

Broad-band spectra (pulsed)

- High-energy (>100MeV) photons are emitted via **curvature** process by ultra-relativistic (~10 TeV) $e^{\pm}$'s accelerated in pulsar magnetosphere.

- Some of such **primary** γ-rays are absorbed in the NS magnetosphere and reprocessed in lower energies via **synchrotron** process.

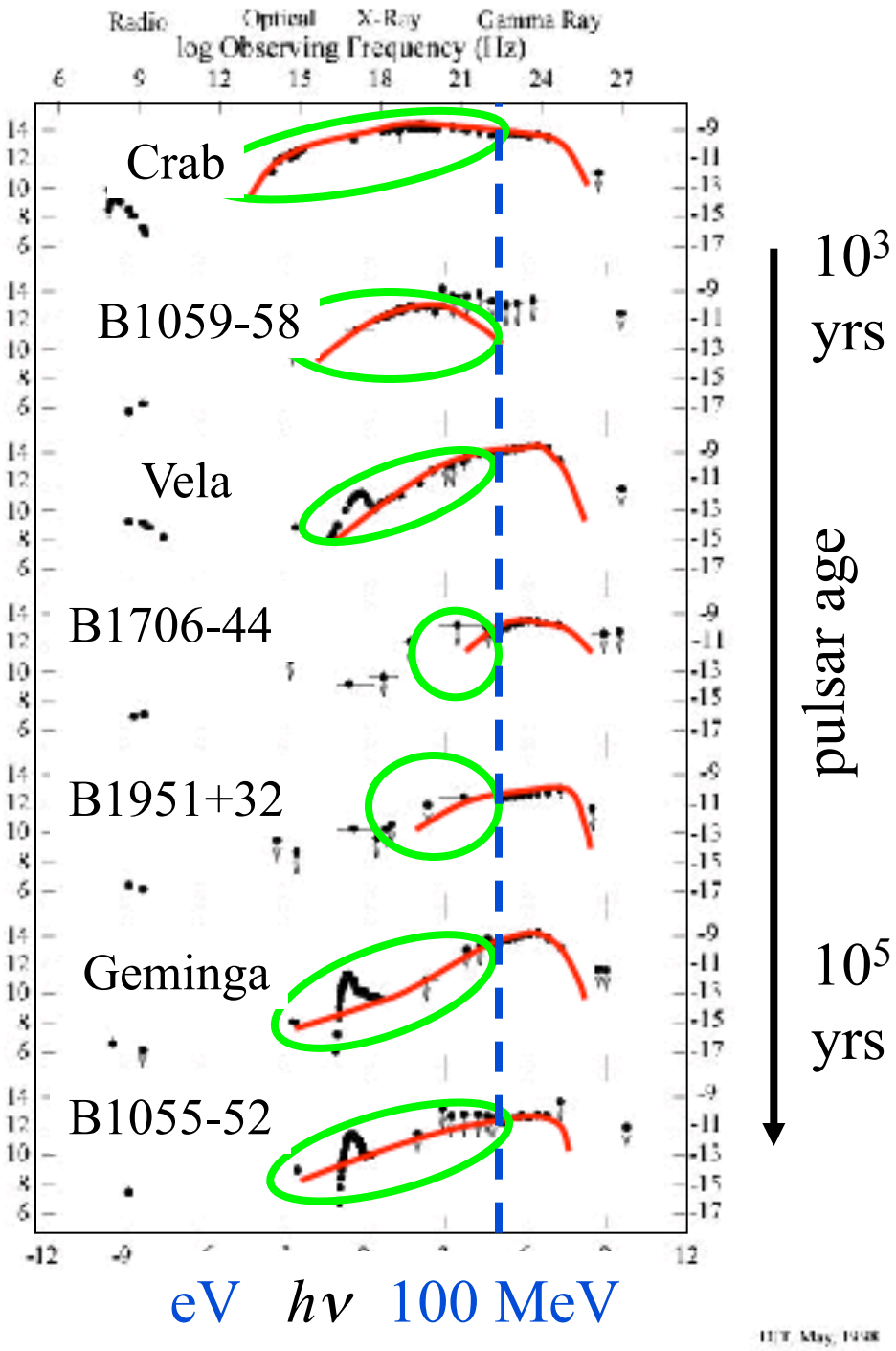

§ 2 *Previous Models*

Early 00's, Muslimov & Harding (2003, ApJ 588, 430) proposed an alternative model, pair-starved PC (PSPC) model, extending the lower-altitude slot-gap model (original: Arons 1983) into higher altitudes.

Due to special relativistic effects, wide-separated double peaks appear (same as in OG model).

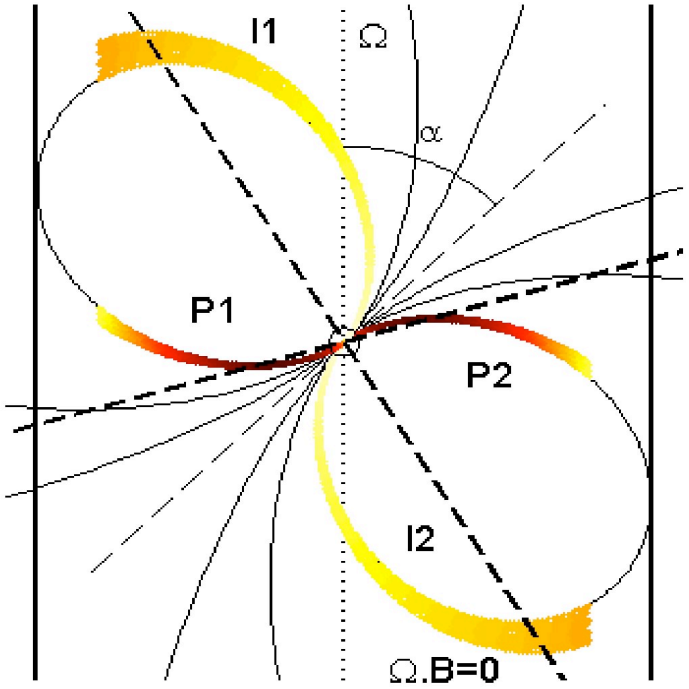

§ 2 *Previous Models*

However, the original idea of geometrically thin PSPC model cannot explain observed flux of γ-ray pulsars.

Hirotani (2008) ApJ 688, L25

In the Crab pulsar (Ω=190 rad s^{-1}):

For OG model (f~0.14, κ~0.3, μ=4×10^{30} G cm^3),

$$(\nu F_\nu)_{\rm peak} \sim 4\times10^{-4}\ {\rm MeV\ s^{-1}\ cm^{-2}} \sim {\rm Fermi\ flux}.$$

For PSPC (or slot-gap) model (f~0.04, κ~0.2, large μ),

$$(\nu F_\nu)_{\rm peak} \sim 3\times10^{-5}\,(\mu/8\times10^{30})^2\ {\rm MeV\ s^{-1}\ cm^{-2}} < 0.1\ {\rm Fermi\ flux}.$$

For other pulsars, thin PSPC (SG) model predicts further small fluxes than (typically < 1% of) observed.

§ 2 *Previous Models*

Various attempts have been made on recent OG model:

3-D geometrical model
→ γ-ray emission morphologies,
phase-resolved spectra (Cheng + ’00; Tang + ‘08)

2-D self-consistent solution (Takata + ’06; Hirotani ‘06)

3-D geometrical model
→ atlas of light curves for PC, PSPC, OG models
(Watters + ’08)

In this talk, I will concentrate on 3-D self-consistent modeling and discuss resulting emission from IR to VHE.

§ 2 Basic Emission Mechanism

A rotating NS magnetosphere can be divided into open and closed zones.

Last-open field lines form the boundary of them.

In the open zone, $e^{\pm}$'s escape through the light cylinder as a pulsar wind.

In the closed zone, on the other hand, an $E_{||}$ would be very quickly screened by the dense plasmas.

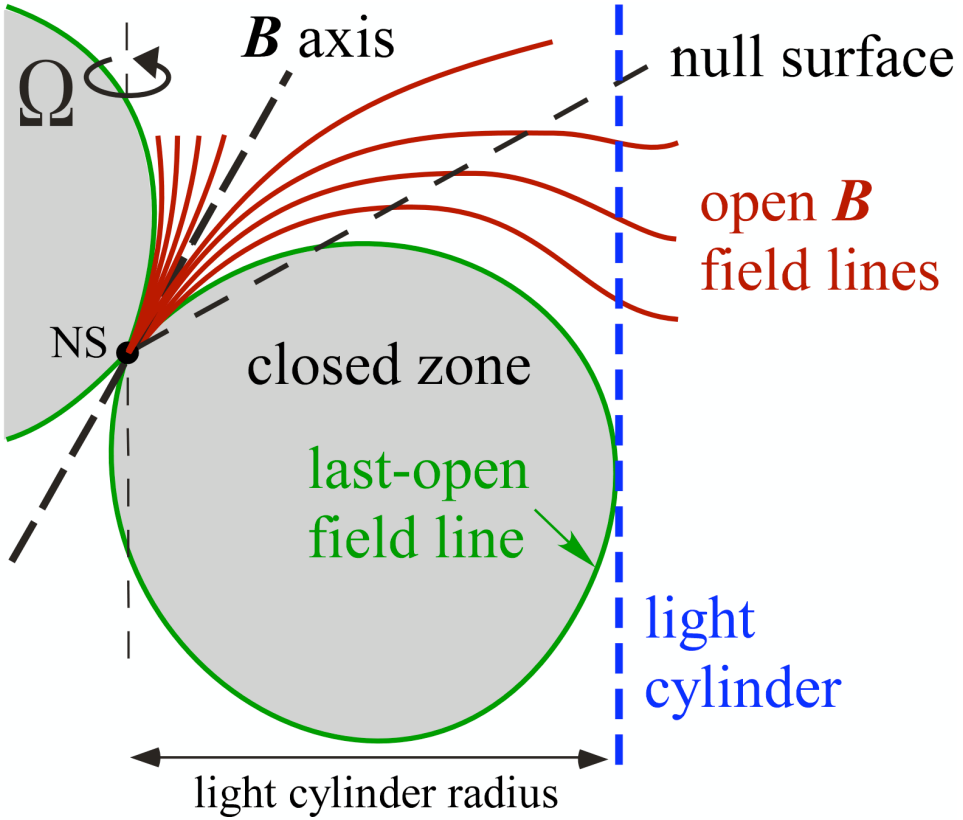

$$\varpi_{LC} = 3\times10^{8}(\Omega/10^{2}\,\mathrm{rad\,s^{-1}})\ \mathrm{cm}$$

§ 2 Basic Emission Mechanism

A rotating NS magnetosphere can be divided into open and closed zones.

Last-open field lines form the boundary of them.

In the open zone, $e^{\pm}$'s escape through the light cylinder as a pulsar wind.

In the closed zone, on the other hand, an $E_{||}$ would be very quickly screened by the dense plasmas.

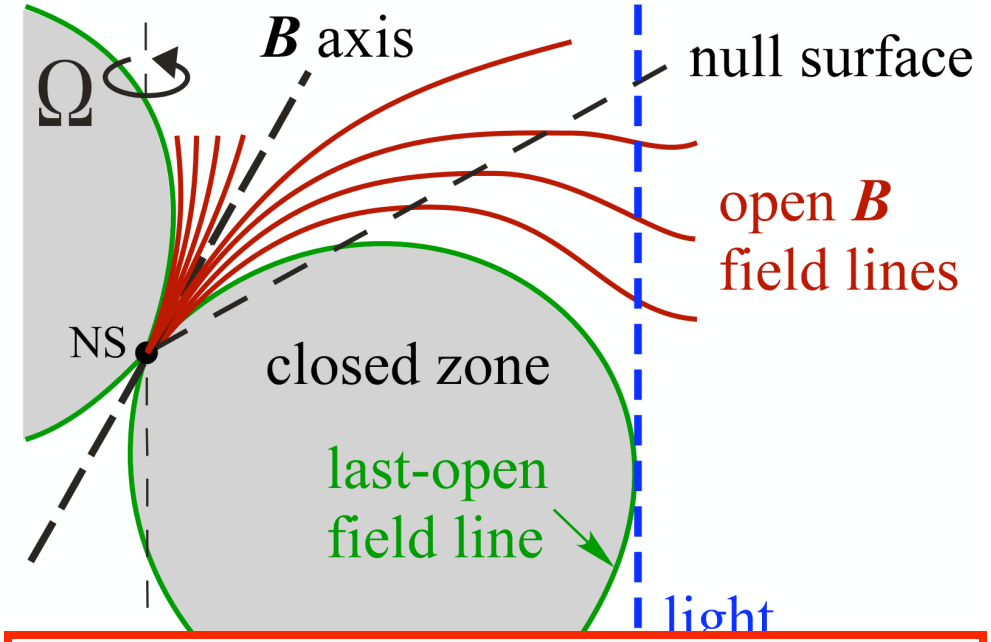

Thus, in all pulsar emission models, particle acceleration takes place only within the open zone.

§ 2 Basic Emission Mechanism

For typical high-energy pulsars, open zone occupies only a few degrees from ***B*** axis on the PC surface.

Available voltage in the open zone:

$$\text{EMF} \sim \frac{\Omega^2 B_* r_*^3}{c^2} \sim 10^{15.5}\ \text{V}$$

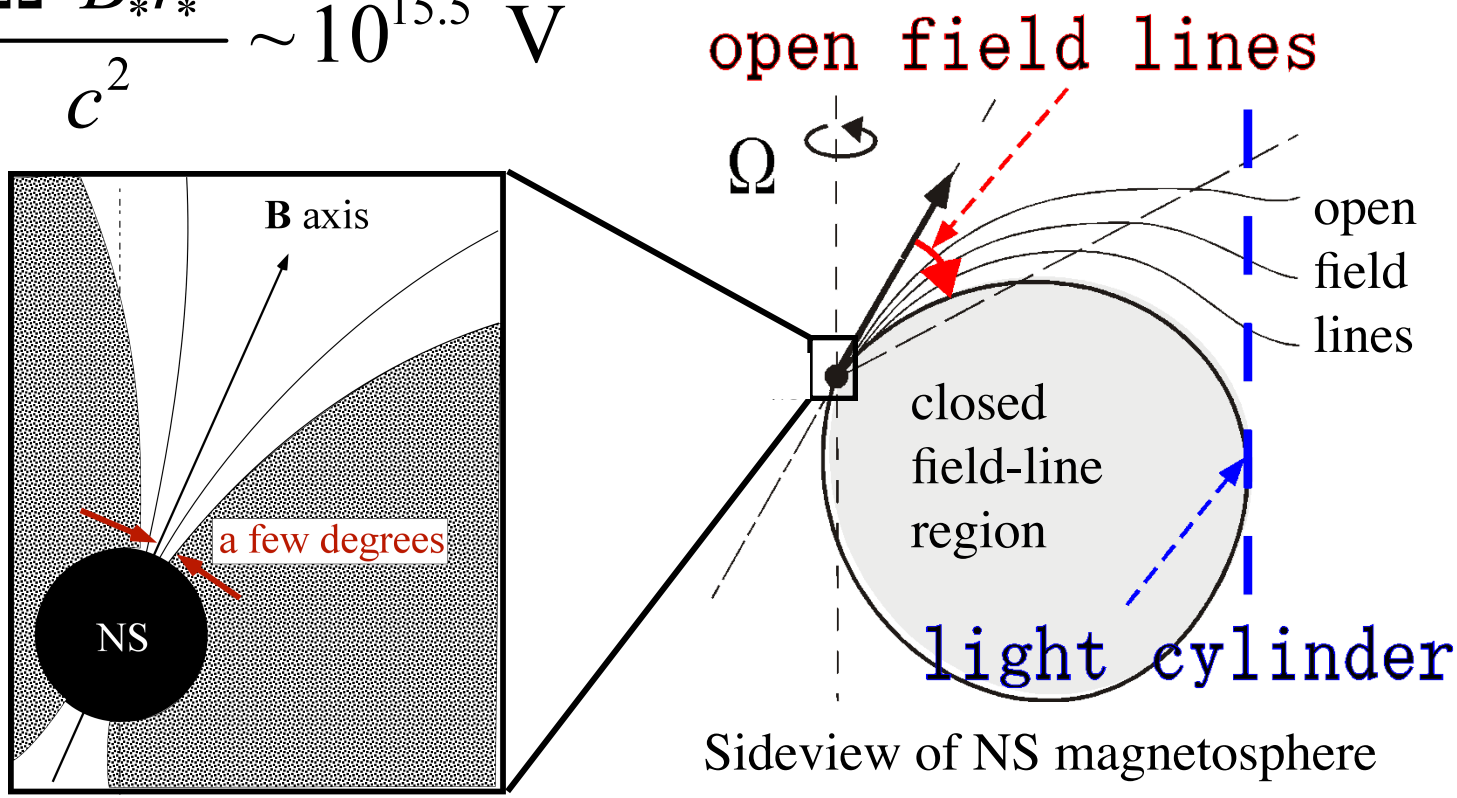

§ 2 Basic Emission Mechanism

In a rotating NS magnetosphere, the Goldreich-Julian charge density is induced for a static observer. The inhomogeneous part of Maxwell eqs. give

$$\nabla \cdot \mathbf{E}_{\parallel} = 4\pi(\rho - \rho_{\mathrm{GJ}}),$$

where $\mathrm{E}_{\parallel} \equiv \mathbf{E}\bullet\mathbf{B}$, $\rho \equiv e(n_{+} - n_{-})$ and

$$\rho_{\mathrm{GJ}} \equiv \frac{1}{4\pi}\nabla \cdot \mathbf{E}_{\perp} = -\frac{\mathbf{\Omega}\cdot\mathbf{B}}{2\pi c}.$$

It follows that $E_{\parallel}$ arises if $\rho \neq \rho_{\mathrm{GJ}}$.

Note that ρ_{GJ} is uniquely determined by B-field geometry. For example, it changes at the so-called 'null-charge surface'.

§ 2 Basic Emission Mechanism

$$\rho_{GJ} \equiv \frac{1}{4\pi}\nabla\cdot\mathbf{E}_{\perp}$$
$$= -\frac{\mathbf{\Omega}\cdot\mathbf{B}}{2\pi c}.$$

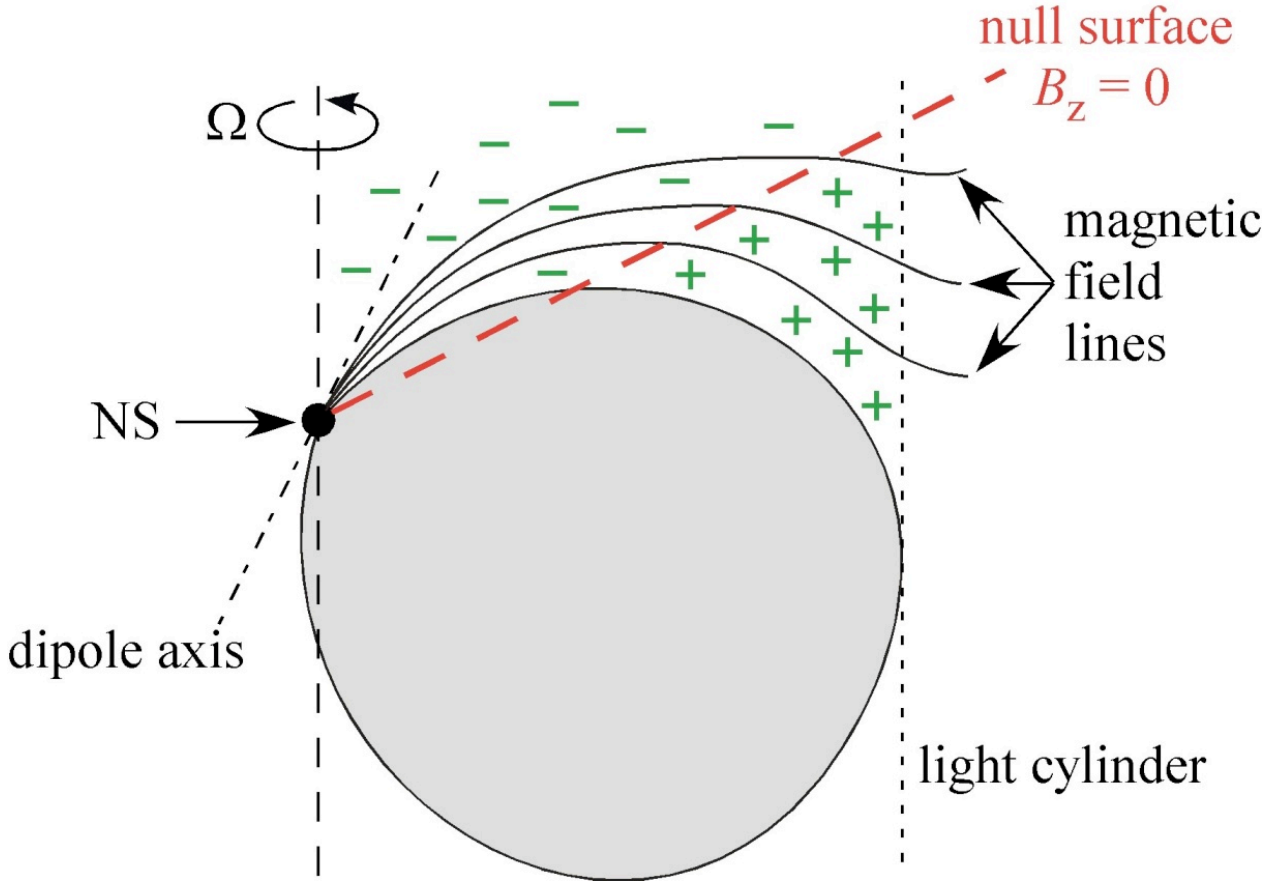

Note that ρ_{GJ} is uniquely determined by B-field geometry. For example, it changes at the so-called 'null-charge surface'.

§3 Emission Models

Next question:

Where is the particle accelerator, in which $\boldsymbol{E}_{\parallel}$ arises?

In this section, we geometrically consider three representative pulsar high-energy emission models:

(historical order)

1. Inner-gap (or polar-cap) model, 1982-1990's
2. Outer-gap model, 1986-present
3. Slot-gap model 2003-2009

Note: Inner-gap model still survives as the only theory that explains coherent radio pulsations.

§ 3 Emission Models

Special relativistic effects in outer magnetosphere:

On the leading side, phase shifts add up to spread photons emitted at various altitudes over 140° in phase.

On the trailing side, photons emitted earlier at lower altitudes catch up with those emitted later at higher altitudes to focus in a small phase range 30°, forming caustics (strong intensity) in the phase plot.

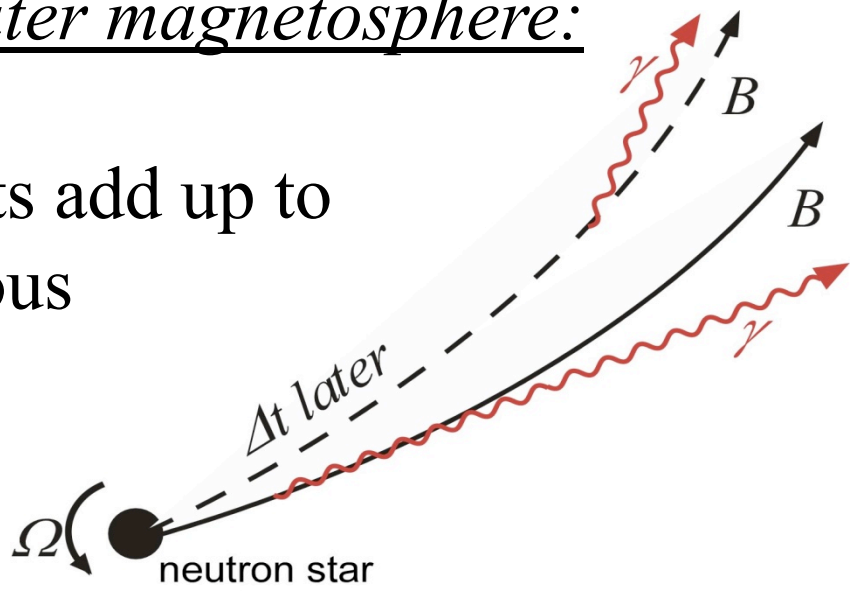

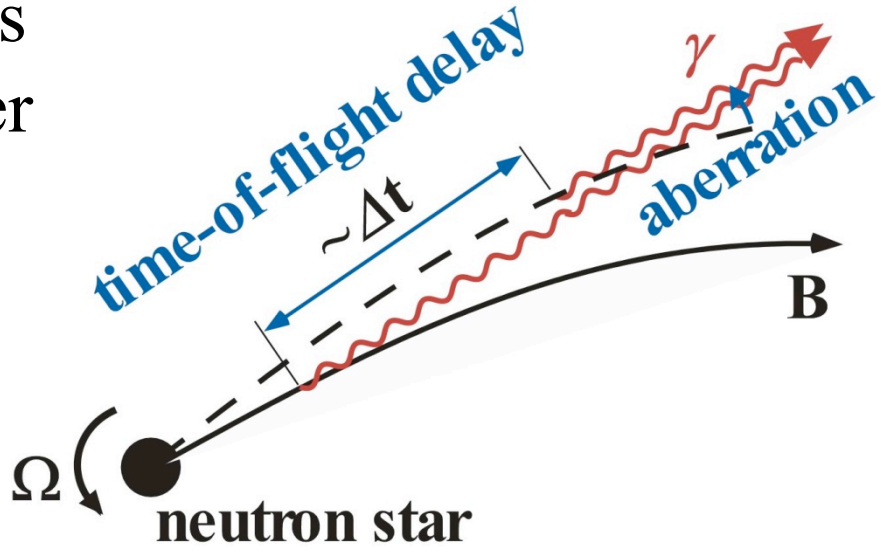

§1 Introduction: The γ-ray sky

The *Large Area Telescope* (20 MeV – 300 GeV) aboard the *Fermi Gamma-Ray Space Telescope*.

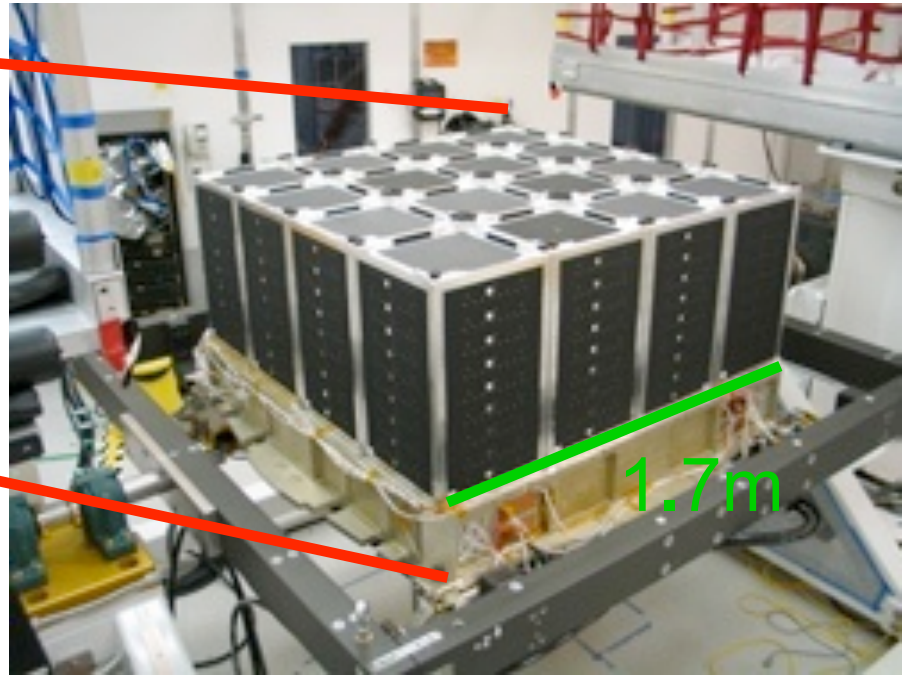

LAT PSF ~ 0.1° @ 1 GeV
FOV ~ 2.5 ster
sensitivity ~ 30*EGRET

§1 Introduction: The γ-ray sky

The *Large Area Telescope* (20 MeV – 300 GeV) aboard the *Fermi Gamma-Ray Space Telescope*.

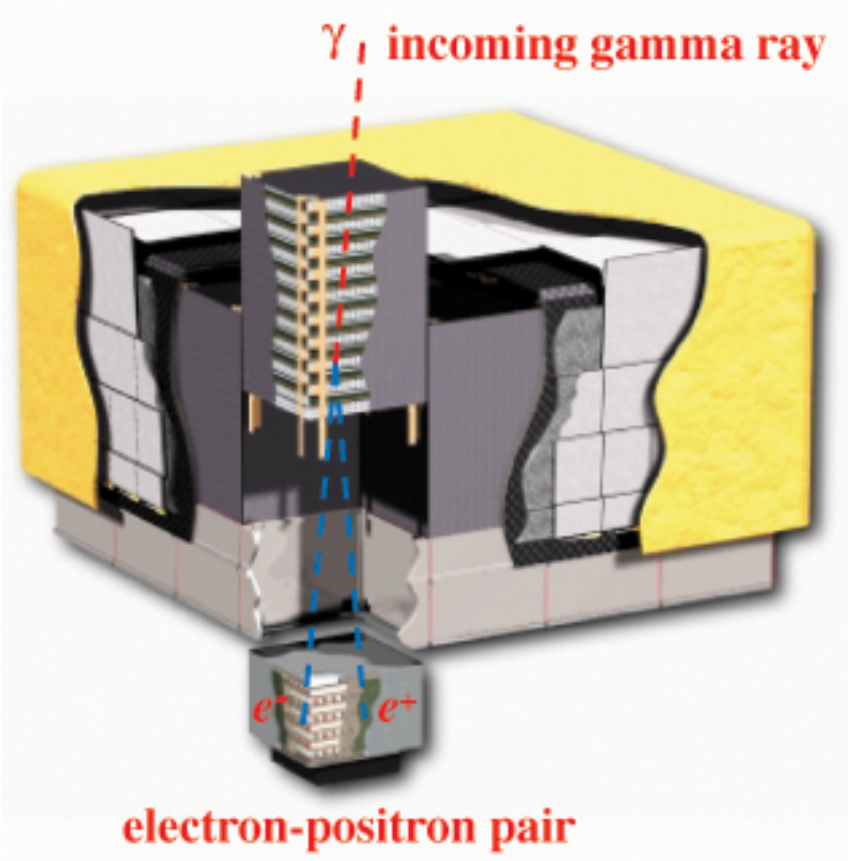

§1 Introduction: CGRO observations

γ-ray pulsars emit radiation in a wide frequency range:

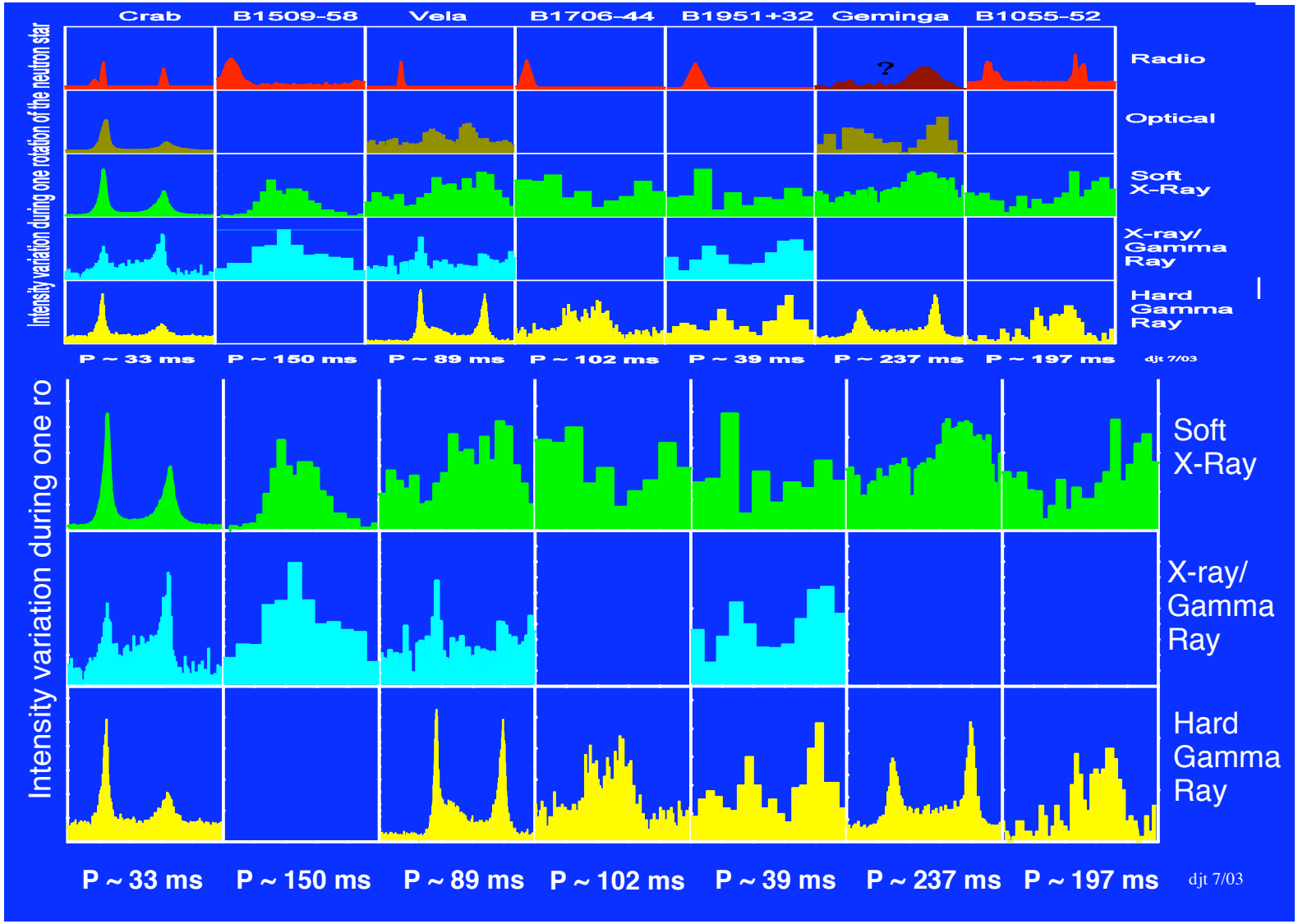

Thompson 2003, astro-ph/0312272